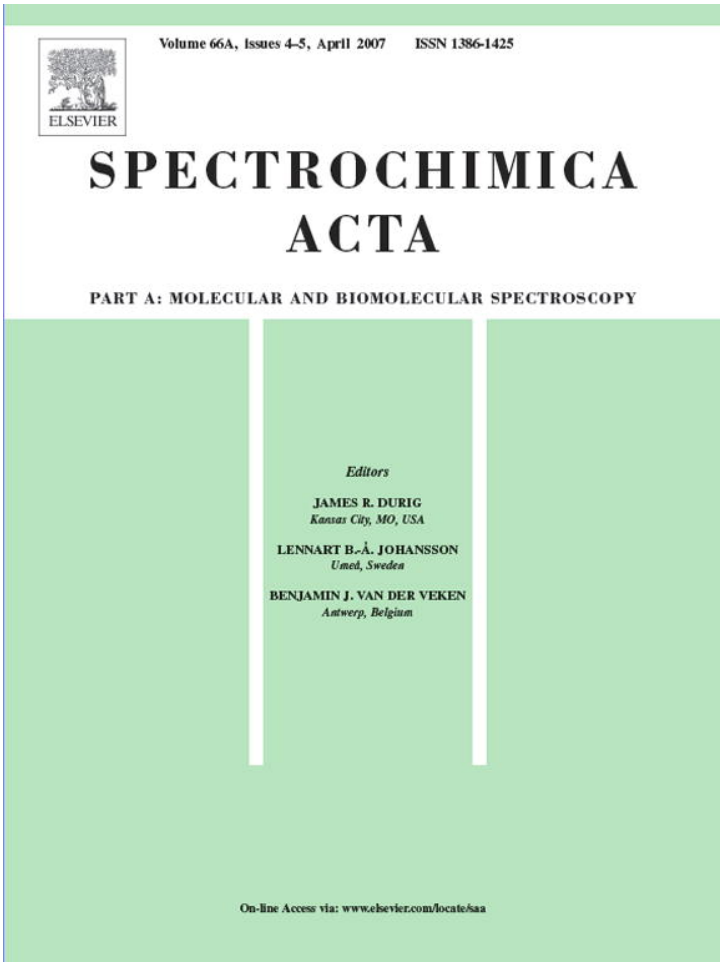

Available online at www.sciencedirect.com
ScienceDirect
Spectrochimica Acta Part A 66 (2007) 884–897
SPECTROCHIMICA ACTA PART A
www.elsevier.com/locate/saa

Experimental and theoretical study of the hydration of phosphate groups in esters of biological interest

S.A. Brandán [a], S.B. Díaz [a], J.J. López González [b], E.A. Disalvo [c,1], A. Ben Altabef [a,*,1]

[a] *Instituto de Química Física, Facultad de Bioquímica, Química y Farmacia, Universidad Nacional de Tucumán, San Lorenzo 456 (4000), Tucumán, Argentina*
[b] *Departamento de Química Física y Analítica, Facultad de Ciencias Experimentales, Universidad de Jaén, Campus de Las Lagunillas, Edif. B-3, E-23071 Jaén, España*
[c] *Laboratorio de Fisicoquímica de Membranas Lipídicas, Facultad de Farmacia y Bioquímica, Universidad de Buenos Aires, Junín 956 2°P. (1113), Buenos Aires, Argentina*

Received 21 September 2005; received in revised form 30 April 2006; accepted 3 May 2006

Abstract

We have studied the influence of different groups esterified to phosphates on the strength of the interaction of the P─O bond with one water molecule. Experimental vibrational spectra of PO_4^{3-}, HPO_4^{2-}, $H_2PO_4^-$, phosphoenolpiruvate (PEP) and ortho-phosphocholamine (*o*-PC) were obtained by means of FTIR spectroscopy. Geometry calculations were performed using standard gradient techniques and the default convergence criteria as implemented in GAUSSIAN 98 Program. In order to assess the behaviour of such DFT theoretical calculations using B3LYP with 6-31G* and 6-311++G** basis sets, we carried out a comparative work for those compounds. The results were then used to predict the principal bands of the vibrational spectra and molecular parameters (geometrical parameters, stabilisation energies, electronic density). In this work, the relative stability and the nature of the P─O bond in those compounds were systematically and quantitatively investigated by means of Natural Bond Order (NBO) analysis.

The topological properties of electronic charge density are analysed employing Bader's Atoms in Molecules theory (AIM). The hydrogen bonding of phosphate groups with water is highly stable and the P─O bond wavenumbers are shifted to lower experimental and calculated values (with the DFT/6-311++G** basis set). Accordingly, the predicted order of the relative stability of the hydrogen bonding of the water molecule to the P─O bond of the investigated compounds is: PO_4^{3-} > HPO_4^{2-} > $H_2PO_4^-$ > phosphoenolpiruvate > phosphocholamine for the two basis sets used.

Keywords: Vibrational spectra; PO_4^{3-}; HPO_4^{2-}; $H_2PO_4^-$; Phosphoenolpiruvate; Ortho-phosphocholamine; Vibrational spectra; Hydrogen bonding

1. Introduction

Phosphates are important intermediates in dissociative mechanisms. Thus, the hydrolysis of phosphates and their structure and stability are of fundamental interest [1–9]. Phosphate is a common chemical group in all the phospholipids composing natural membranes [10,12]. It is linked to the acyl glycerol backbone and esterified to charged and uncharged chemical groups such as, choline, ethanolamine, glycerol and others.

The phosphate group has been identified as the primary region of hydration [13,14]. The mobility of the phosphate increases with hydration reaching a constant value at around six water molecules per lipid. Thus, the first six water molecules are believed to constitute the first hydration layer bound to the oxygen phosphates and ester bonds.

The phosphate hydration can be followed by the vibrational frequency shift of the P–O antisymmetric mode [1,2,4,15]. Exposure of lipids to dehydration by heat-drying and by osmotic stress promotes a shift of the PO_2^- frequency to higher values, denoting the displacement of water molecules [13,14]. This observation is very important due to relevance in the biological function and stability of membranes under hydric stress [15–20].

* Corresponding author. Tel.: +54 381 4311044; fax: +54 381 4248169.
[1] They are members of the Research Career of CONICET (National Research Council of Argentina).

1386-1425/$ – see front matter © 2006 Elsevier B.V. All rights reserved.
doi:10.1016/j.saa.2006.05.005

In addition, polyhydroxilated compounds such as trehalose or phloretin, may compete with water, binding to the phosphate and displacing the frequency to lower values. This is taken as an evidence that the H-bond formed by the OH groups of these compounds is stronger than the H-bond of water with the PO_2^-.

Phloretin decreases the dipole potential, a potential built at the membrane interface by the orientation of constitutive and water dipoles. As FTIR measurements show that phloretin strongly interacts with the PO_2^- group, but not with carbonyls, it has been suggested that this compound eliminates polarised water from this group. The effectiveness of phloretin to decrease the dipole potential of monolayers in the fluid state is lessened by the moieties esterified to the phosphate group in the sequence choline > ethanolamine > glycerol [16].

Thus, it is important to notice that the effect of phloretin on the dipole potential is modulated by the group which the phosphoacyl glycerol is esterified to. However, the relation of this effect with the binding energy of the water molecules to the phosphate PO_2^- group in each of the compounds it is not clear.

Taking into account that the insertion of OH compounds (HOX) in the hydration site of the PO_2^- group may follow a sequence such as:

$$RO–P{=}O–HOH \rightarrow RO–P{=}O + HOH \quad (1)$$

$$RO–P{=}O + HOX \rightarrow RO–P{=}O\cdots HOX \quad (2)$$

it is reasonable to think that the step of dehydration (1) may depend on the group R to which the phosphate is esterified.

The purpose of this paper is to study the influence of esterified groups (R) to the phosphate (PO_2^-) on the strength of the P–O interaction with a water molecule in order to elucidate the energetic contribution of step (1) in the interaction of polyhydroxilated compounds with different phospholipids.

With this aim, we have chosen compounds of the general formula $RR'(PO_4)^- Na^+$ in which R=H and R′ is substituted by H, enolpiruvate or cholamine and analysed their FTIR and Raman spectra.

Geometry calculations were performed using standard gradient techniques and the default convergence criteria as implemented in GAUSSIAN 98 Program [21]. In order to assess the behaviour of such theoretical calculations, we have made a comparative work for those compounds using DFT/B3LYP method with 6-31G* and 6-311++G** basis sets. The relative stability and the nature of the P–O bond in those compounds were systematically and quantitatively investigated by the NBO analysis [22–24].

The study of model phosphates is very important to understand the impact of unusual bonding on the properties of such molecules. In addition, from the AIM [25] analysis of different compounds, the electron density value for the PO bond and the hydrogen bond were studied. The occupancies for the PO bonding and antibonding orbitals have also been predicted by NBO analysis [22–24]. The basic idea in the natural atomic orbitals (NAO) and NBO analysis could be briefly described as the use of one-electron density matrix to define the shape of the atomic orbital in the molecular environment and derive molecular bonds from electron density between atoms. The importance of quantum mechanical orbital interaction and the exchange effects were evaluated. Charge transfer (CT) from one of the oxygen lone pairs, n, of the electron donor to the proximate OH antibond, σ*, of the electron acceptor was found to be of critical importance in all studied compounds.

The general importance of $n \rightarrow \sigma^*$ and other forms of CT stabilisation in intermolecular interactions have been examined by NBO analysis, using optimised intermolecular geometry. In the present work, we have found that charge transfer effects are highly significant in the studied compounds.

2. Materials and methods

$Na_3PO_4{\cdot}12H_2O$, $Na_2HPO_4{\cdot}12H_2O$, $NaH_2PO_4{\cdot}H_2O$, phosphoenolpyruvic acid monosodium monohydrate ($HOOCC(CH_2)OPO_3HNa{\cdot}H_2O$), *o*-phosphocholamine, ($NH_2CH_2CH_2OPO_3H_2$) were obtained from Fluka BioChemika.

The infrared spectra of the compounds were obtained in KBr pellets at room temperature between 4000 and 400 cm^{-1} on a FTIR Perkin-Elmer Model 1600 spectrophotometer, equipped with a Globar source and DTGS detector. Fig. 1a shows the FTIR spectrum of solid ortho-phosphocholamine (*o*-PC) while Fig. 1b shows the FTIR spectrum of phosphoenolpiruvate (PEP).

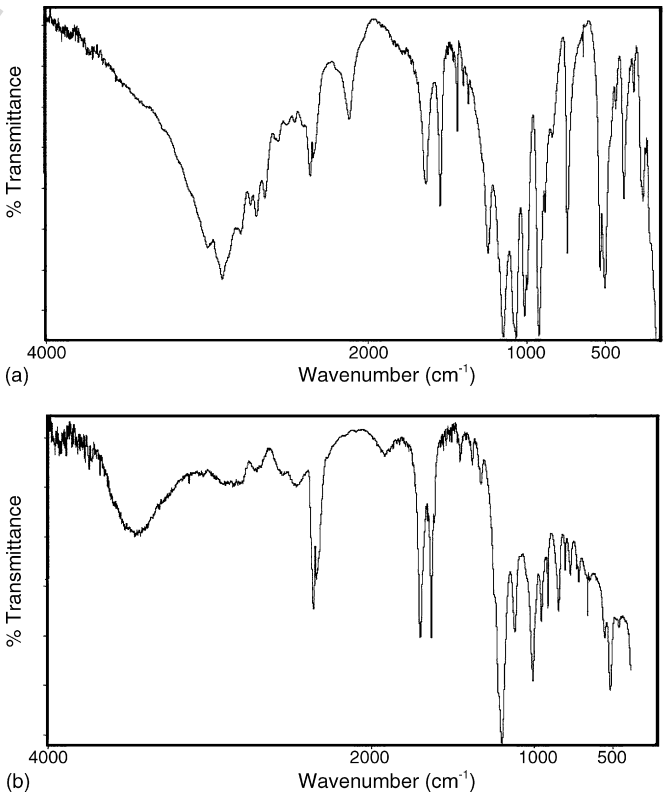

Fig. 1. (a) FTIR spectrum in solid phase of *o*-phosphocholamine between 4000 and 400 cm^{-1}, resolution 1 cm^{-1}. (b) FTIR spectrum in solid phase of phosphoenolpyruvic acid monosodium monohydrate between 4000 and 400 cm^{-1}, resolution 1 cm^{-1}.

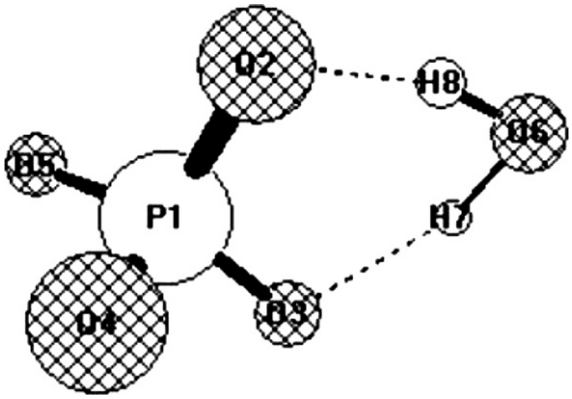

Fig. 2. The molecular structure of PO_4^{3-} (H_2O).

2.1. Computational details

All calculations were made using the GAUSSIAN 98 [21] set of programs running on a PC Pentium III working under a Linux operative system. Geometry calculations were performed using standard gradient techniques and the default convergence criteria as implemented in GAUSSIAN. Initial structures for PO_4^{3-}, HPO_4^{2-}, $H_2PO_4^{-}$, phosphoenolpiruvate (PEP) and ortho-phosphocholamine (*o*-PC) compounds were modelled without and with one water molecule and with the *Gauss-View* program [26]. These initial geometries used for all studied compounds were optimised by a functional Becke's three parameter exchange and the non-local correlation provided by Lee-Yang-Parr's (B3LYP) [27,28] using 6-31G* and 6-311++G** basis sets. The choice of these basis sets, specially the 6-311++G** basis set, is based on satisfactory results obtained in previous studies on biological metaphosphate, phosphate and phosphoborane compounds [3]. These structures of the studied species with one water molecule are observed in Figs. 2–6. The nature of the stationary points was checked by calculating the vibrational wavenumbers. NBO analysis was then performed using the same basis set by the NBO 3.1 program [29,30] included in GAUSSIAN 98 package programs [21].

The topological properties of the charge density in all systems studied were computed with the AIM2000 software [31].

3. Results and discussion

3.1. Geometrical parameters

The optimised structure with the B3LYP/6-31G* and B3LYP/6-311++G** methods for PO_4^{3-} ion has a T_d symmetry while the PO_4^{3-} (H_2O) complex has a C_{2v} symmetry as in other papers reported [1,2]. The optimised structure for HPO_4^{2-} ion and its corresponding hydrated complex, HPO_4^{2-} (H_2O) has C_s symmetry. In this case, the structure of HPO_4^{2-} ion is different from that proposed initially by Chapman and Thirlwell [8] and then by Niaura et al. [9] where the OH group is treated as a point mass with C_{3v} symmetry. The optimised structure of $H_2PO_4^{-}$ ion and its corresponding hydrated complex, $H_2PO_4^{-}$ (H_2O) has C_2 symmetry. Also, in this case the OH groups are not taken as punctual masses with C_{2v} symmetry [8,9]. The water molecules

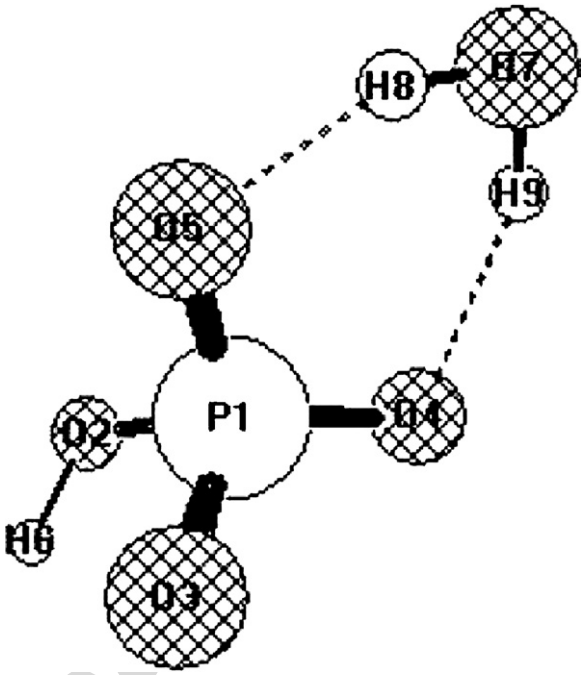

Fig. 3. The molecular structure of HPO_4^{2-} (H_2O).

of all phosphate complexes have a bidentate structure. Table 1 shows the comparison between total energy values for PO_4^{3-} and PO_4^{3-} (H_2O) and the values obtained by Pye et al. [2] using the HF/6-31G* and HF/6-31+G* methods. It should be notice that in all cases, lower energies are obtained using DFT methods combined with a diffuse function basis set. The total energies for the remaining uncomplexed and hydrated compounds are given in Table 2. In the potential energy surface of PEP (H_2O) complex we observed two structures with C_S and C_1 symmetries, but the first structure has an imaginary frequencies therefore the geometrical parameters were calculated with C_1 symmetry. In

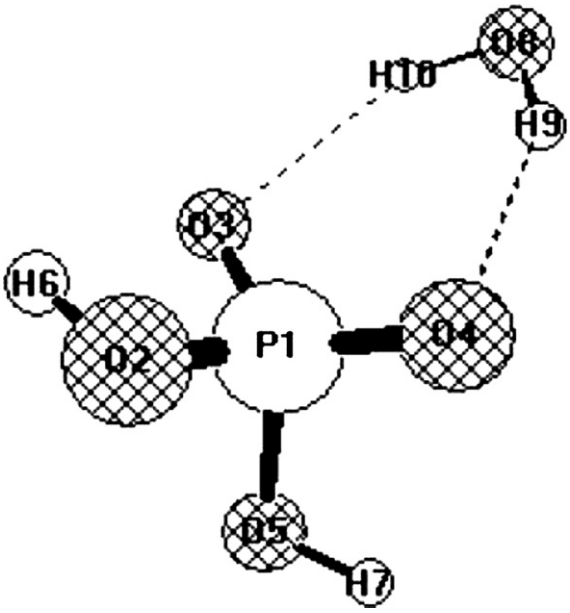

Fig. 4. The molecular structure of $H_2PO_4^{-}$ (H_2O).

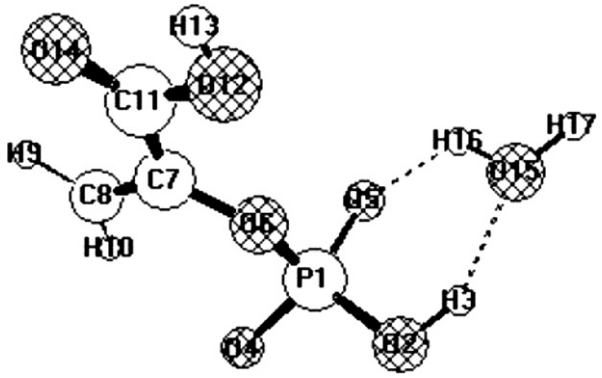

Fig. 5. The molecular structure of phosphoenolpyruvate hydrated with one water molecule.

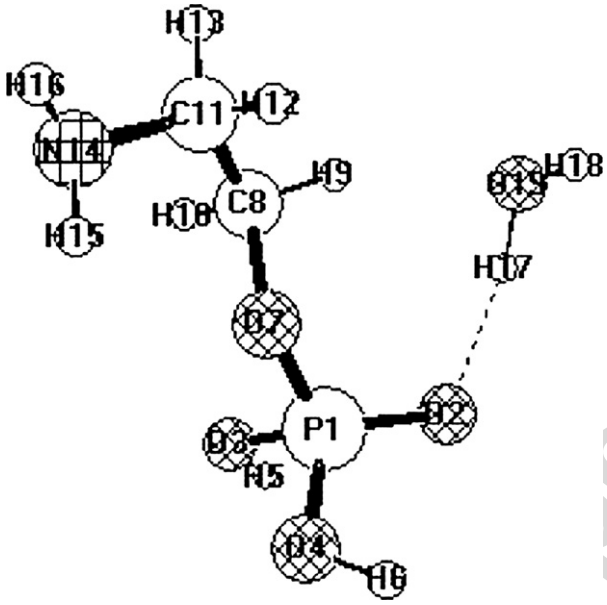

Fig. 6. The molecular structure of *o*-phosphocholamine hydrated with one water molecule.

the complex with C_s symmetry, the water molecule is bidentate while in the one with C_1 symmetry is monodentate. The same observation can be made for the *o*-PC (H_2O) complex.

Table 3 shows the distances at B3LYP level using 6-31G* and 6-311++G** basis sets for PO_4^{3-} and PO_4^{3-} (H_2O) compared with other results obtained from the literature [1,2]. Geometrical parameters at different levels of theory for HPO_4^{2-} (H_2O), $H_2PO_4^-$ (H_2O), PEP (H_2O) and *o*-PC (H_2O) complexes are given in Table 4. Our results with 6-31G* basis set show that the

Table 2
Total energies (a.u.)[a] at different levels of theory for the compounds without and hydrated with one water molecule

	B3LYP 6-31G*[b]	B3LYP 6-311++G**[b]
HPO_4^{2-} (C_s)	−642.8175	−643.0178
HPO_4^{2-} (H_2O) (C_s)[c]	−719.2883	−719.5265
HPO_4^{2-} (H_2O) (C_1)[c]	−719.2890	−719.5256
$H_2PO_4^-$ (C_2)	−643.5876	−643.7536
$H_2PO_4^-$ (C_s)	−643.5862	−643.7520
$H_2PO_4^-$ (H_2O) (C_2)[c]	−720.0285	−720.2376
PEP (C_1)	−909.5592	−909.7985
PEP (H_2O) (C_S)[c]	−985.9947	−986.2762
PEP (H_2O) (C_1)[d]	−985.9998	−986.2790
o-PC (C_1)	−778.0981	−778.2873
o-PC (H_2O) (C_s)[c]	−854.5061	−854.7424
o-PC (H_2O) (C_1)[d]	−854.5212	−854.7564
o-PC (H_2O) (C_1)[d]	−854.5226	−854.7584

[a] a.u. = atomic units.
[b] This work.
[c] Water bidentate.
[d] Water monodentate.

P–O (free) in PO_4^{3-} (H_2O) (1.5785 Å) decreases in connection with PO_4^{3-} (1.5990 Å) (Table 3), whereas the P–O (bound) distance (1.6131 Å) increases as observed by Pye et al. [2] in Hartree Fock calculations (1.5782 Å). A similar result is observed in all studied complexes with the same basis set. The H-bond weakens the P–O bond slightly while the strength of the P–O (free) bond decreases in the hydrated PO_4^{3-}, HPO_4^{2-} and PEP complexes. The geometrical parameters of PO_4^{3-} (H_2O) complex calculated with DFT method somewhat overestimates the experimental bond length of 1.55 Å [1,11] in relation to Hartree Fock calculations. This same difference for PO_4^{3-} (H_2O) was observed by Ebner et al. [1] with B3LYP/6-311+G** method. The O···H, P···O (H_2O) and O···O distances in PO_4^{3-} (H_2O) (see Table 3) are lower with the DFT methods compared with the corresponding HF methods. Only the O–H (H_2O) distance with B3LYP method is longer than the obtained values with ab initio methods [2]. In HPO_4^{2-} (H_2O) the P–O (free) distance decreases with the 6-31G* basis set calculations whereas it increases with 6-311++G** basis set calculations. In the $H_2PO_4^-$ (H_2O) complex a slight increase of the P–O (bound) distance in reference to the P–O (free) distance (1.5005 Å) is observed with a greater value in the O···H distance (2.0375 Å with B3LYP/6-31G* and 2.1033 Å with B3LYP/6-311++G**). In this case, P–O (free) means P–O (bond OH) it is connected to

Table 1
Total energies (a.u.)[a] at different levels of theory for PO_4^{3-} and PO_4^{3-} (H_2O)

	HF 6-31G*[b]	HF 6-31+G*[b]	B3LYP 6-31G*[c]	B3LYP 6-311++G**[c]
PO_4^{3-} (T_d)	−639.7078	−639.8131	−641.8124	−642.0874
PO_4^{3-} (H_2O) (C_{2v})[d]	−715.8090	−715.9036	−718.3294	−718.6247

[a] a.u. = atomic units.
[b] Pye et al. [2].
[c] This work.
[d] Water bidentate.

Table 3
Geometrical parameters (distances in Å) for PO_4^{3-} (H_2O) at different levels of theory

PO_4^{3-} (H_2O)	HF 6-31G*[a]	HF 6-31+G*[a]	B3LYP 6-311+G**[b]	B3LYP 6-31G*[c]	B3LYP 6-311++G**[c]
P—O (free)	1.5510	1.5577	–	1.5785	1.5829
P—O (bound)	1.5782	1.5790	1.6700	1.6131	1.6133
O···H	1.7617	1.8218	1.7090	1.6891	1.7155
O—H (H_2O)	0.9868	0.9811	1.0250	1.0295	1.0166
O(PO_4^{3-})···O (H_2O)	2.6881	2.7283	–	2.6716	2.6698
P···O (H_2O)	3.3086	3.3615	–	3.2973	3.3168
PO_4^{3-} P—O (free)	1.5673	1.5718	–	1.5990	1.5990

[a] Pye et al. [2].
[b] Ebner et al. [1].
[c] This work.

the H atom of the $H_2PO_4^-$ (H_2O). The strength of the H-bond is higher in the PO_4^{3-} (H_2O) complex (1.6891 Å) and decreases in the HPO_4^{2-} (H_2O) (1.8513 Å) and $H_2PO_4^-$ (H_2O) (2.0375 Å) complexes.

These variations can be observed studying the bond orders and the atomic charges of the complexes. The bond order, expressed as Wiberg indexes and atomic charges of the phosphates complexes with one water molecule and the corresponding to *o*-PC and PEP complexes with one water molecule are given in Tables S1 and S2 of the Supporting Information. When the charge of O atom of the P–O bond involved in the formation of H-bond of the different complexes is analysed, the trend, with the two basis sets used, is that the charge on the O atom decreases when the bond order increases in the following order: PO_4^{3-} (H_2O) > HPO_4^{2-} (H_2O) > $H_2PO_4^-$ (H_2O) > *o*-PC (H_2O). This variation agrees with the strength of the H-bond because it is greater in the PO_4^{3-} (H_2O) complex and lower in the *o*-PC (H_2O) complex. The exception in the PEP complex occurs because the charge of O atom decreases(−0.713567 with 6-31G* basis set at −0.457783 with 6-311++G** basis set) when the bond order increases from 3.5606 (6-31G*) at 3.6325 (6-311++G**).

Table 4
Geometrical parameters (distances in Å) for HPO_4^{2-} (H_2O), $H_2PO_4^-$ (H_2O), PEP (H_2O) and *o*-PC (H_2O) at different levels of theory

	B3LYP 6-31G*	B3LYP 6-311++G**
HPO_4^{2-} (H_2O)		
P—O (free)	1.5419	1.5435
P—O (bound)	1.5481	1.5468
P—O (bound OH)	1.7552	1.7576
O···H	1.8513	1.8824
O—H (H_2O)	0.9949	0.9883
O(PO_4^{3-})···O (H_2O)	2.7713	2.7833
P···O (H_2O)	3.3023	3.3310
HPO_4^{2-} P—O (free)	1.5554	1.5395
$H_2PO_4^-$ (H_2O)		
P—O (bound)	1.5092	1.5049
P—O (bound OH)	1.6679	1.6664
O···H	2.0375	2.1033
O—H (H_2O)	0.9782	0.9722
O(PO_4^{3-})···O (H_2O)	2.9137	2.9610
P···O (H_2O)	3.3142	3.3615
$H_2PO_4^-$ P—O (free)	1.5005	1.5005
PEP (H_2O)		
P—O (free)	1.4931	1.4898
P—O (bound)	1.5184	1.5137
P—O (bound OH)	1.6332	1.6342
O···H	1.6931	1.6992
O—H (H_2O)	1.0044	0.9961
O(PO_4^{3-})···O (H_2O)	2.6504	2.6627
P···O (H_2O)	3.3343	3.4206
PEP P—O (R)	1.7173	1.7124
PEP P—O (free)	1.4950	1.4921
o-PC (H_2O)		
P—O (bound)	1.4890	1.4852
P—O (bound OH)	1.6119	1.6058
O···H	1.8941	1.8641
O—H (H_2O)	0.9786	0.9738
O(PO_4^{3-})···O (H_2O)	2.8441	2.8059
P···O (H_2O)	3.7443	3.7939
o-PC P—O (R)	1.5877	1.5844
o-PC P—O (free)	1.4802	1.4779

Another important observation may be reported about the P atom charge in the different complexes. In general, the trend with the 6-31G* basis set is that increases the P atom charge as the bond orders decrease: PO_4^{3-} (H_2O) > HPO_4^{2-} (H_2O) > $H_2PO_4^-$ (H_2O) > PEP (H_2O) > *o*-PC (H_2O), while with the 6-311++G** basis set the P atom charges decreases with the bond orders in the same direction. The PEP complex with the 6-311++G** basis set is an exception because the P atom charge increases, respect to $H_2PO_4^-$, with the bond order decreases. This variation is probably due this increment in the basis set size decreases the p character of the P atom from 2.44 (6-31G*) to 2.41 (6-311++G*) as Table 5 shows. The above exceptions could occur because the nature of the H-bond in the PEP complex is different from the remaining complexes, (P–OH···O). Thus, the most significant changes could take place in the PO–H bond instead of the P–OH bond.

When the bond order of the O and H atoms of the H_2O molecules involved in the formation of H-bond are analysed, with two basis sets used, the bond order of O atom increases when the bond order of H atom decreases in the following form: PO_4^{3-} (H_2O) > HPO_4^{2-} (H_2O) > $H_2PO_4^-$ (H_2O) > *o*-PC (H_2O). Here again the exception in the PEP complex could be explained by the above reasons.

When using the B3LYP/6-31G* method in *o*-PC complex, the P–O (bound) distance is slightly longer (1.4890 Å) than the P–O (free) (1.4802 Å) and has a smaller value than the other hydrated complexes. Hence, the bond order of the P–O

Table 5
Calculated natural hybrids (NHOs) on P─O positions, polarisation coefficients (C_P, C_O) of each hybrid in the corresponding NBO (in parentheses) and calculated valence non-Lewis, Rydberg non-Lewis, σP─O and σ*P─O bond orbital occupancies

	PO_4^{3-} (H_2O)	HPO_4^{2-} (H_2O)	$H_2PO_4^-$ (H_2O)	PEP (H_2O)	*o*-PC (H_2O)
B3LYP/6-31G*					
Bond P─O (bound)	P─O	P─O	P─O	P─O	P─O
p character P atom	$Sp^{2.97}$	$Sp^{2.58}$	$Sp^{2.36}$	$Sp^{2.44}$	$Sp^{2.41}$
Polarisation coefficient (P)	(0.4626)	(0.4788)	(0.4906)	(0.4852)	(0.4813)
p character O atom	$Sp^{2.41}$	$Sp^{2.22}$	$Sp^{2.18}$	$Sp^{2.26}$	$Sp^{2.31}$
Polarisation coefficient (O)	(0.8866)	(0.8779)	(0.8714)	(0.8744)	(0.8766)
Valence non-Lewis	0.95995	0.88945	0.78235	1.56665	0.92515
Rydberg non-Lewis	0.29027	0.26586	0.24870	0.31348	0.13921
σP─O	1.97755	1.97686	1.97823	1.97526	1.96806
σ*P─O	0.19653	0.16135	0.12943	0.14105	0.11526
B3LYP/6-311++G**					
Bond P─O (bound)	P─O	P─O	P─O	P─O	P─O
p character P atom	$Sp^{3.04}$	$Sp^{2.55}$	$Sp^{2.33}$	$Sp^{2.41}$	$Sp^{2.25}$
Polarisation coefficient (P)	(0.4892)	(0.5007)	(0.5106)	(0.5043)	(0.5121)
p character O atom	$Sp^{2.82}$	$Sp^{2.37}$	$Sp^{2.26}$	$Sp^{2.28}$	$Sp^{2.17}$
Polarisation coefficient (O)	(0.8722)	(0.8656)	(0.8598)	(0.8635)	(0.8589)
Valence non-Lewis	0.70302	0.71000	0.67164	1.41403	0.77315
Rydberg non-Lewis	0.27465	0.24036	0.23797	0.32988	0.26471
σP─O	1.98465	1.98545	1.98554	1.98170	1.98569
σ*P─O	0.15077	0.13094	0.11128	0.12379	0.09670

PEP: phosphoenolpiruvate; *o*-PC: ortho-phosphocholamine.

(bound) in *o*-PC (1.4881) is higher than the other phosphate complexes. For the same compound the value of P–O (bound) with 6-311++G** basis set increases from 1.4779 Å when it is anhydrous to 1.4852 Å when it is hydrated. In this complex longer O···H and P···O (H_2O) distances are observed, in the first one: 1.8941 Å with B3LYP/6-31G* and 1.8641 Å with B3LYP/6-311++G** and, in the second one: 3.7443 Å with B3LYP/6-31G* and 3.7939 Å with B3LYP/6-311++G**. In spite of the higher P–O (bound) value in PEP complex (1.5184 Å) compared with the value in the *o*-PC complex (1.4890 Å), the bond order of O atom in the first complex is higher (1.5389) than the second one (1.4881). In both cases the H-bond is different: in the PEP complex it is of the P–O···H type while in *o*-PC complex it is of the P–OH···O kind. Moreover, the p character of the O atom in the PEP complex is higher (2.28) than in the *o*-PC complex (2.17) as can be seen in Table 5. The greater variation in the P–O (bound) distance with the 6-31G* basis set is observed in the hydrated PO_4^{3-} and in the PEP complexes (0.0014 and 0.0234 Å, respectively). The smaller values are observed in the O(PO_4^{3-})···O (H_2O) distance (2.6716 and 2.6504 Å in PO_4^{3-} and PEP complexes, respectively) and O···H distance (1.6891 and 1.6931 Å in PO_4^{3-} and PEP complexes, respectively). In both complexes, the O···H (H_2O) bound is greater than the values (1.0295 Å and 1.0044 Å in PO_4^{3-} and PEP complexes, respectively) of the other complexes.

It is important to notice that the P–O (bound OH) distances calculated with the 6-31G* and 6-311++G** basis sets, are greater in the hydrated HPO_4^{2-} complex with values of 1.7552 and 1.7576 Å, respectively, while in the hydrated $H_2PO_4^-$ complex they are 1.6679 and 1.6664 Å, respectively. In the hydrated PEP complex the same distance calculated with the 6-31 G* basis set is 1.6332 Å while with the 6-311++G** basis set it is 1.6342 Å. In the hydrated *o*-PC complex the P–O (bound OH) distances estimate with the 6-31G* and 6-311++G** basis sets are 1.6119 Å and 1.6058 Å, respectively. The P–O (R) distance in the hydrated PEP and *o*-PC complexes decreases when the numbers of H atom and the R group increase in the structure. The observed values for the *o*-PC complex estimate with the 6-31G* and 6-311++G** basis sets (1.5877 and 1.5844 Å, respectively) are lower than the corresponding values for the PEP complex (1.7173 and 1.7124 Å, respectively). These observations probably are due to the presence of one P–OR group and two P–OH group in the *o*-PC structure. For the hydrated HPO_4^{2-} complex the distance is even greater (1.7552 Å) because there is one P–OH group.

In general, the variations observed in the distances calculated with 6-311++G** basis set are lower in PO_4^{3-} complex of the order 0.001 Å whereas in the other complexes they are about 0.01 Å.

3.2. NBO analysis method

The calculated natural hybrids (NHOs) on P–O positions, the polarisation coefficients (C_P, C_O) of each hybrid in the corresponding NBO and calculated valence non-Lewis, Rydberg non-Lewis, σP–O and σ*P–O bond orbitals are shown in Table 5. In general, when the p character of P atom NHO of σP–O bond orbital for the phosphate complexes decreases, the p character of O atom NHO of σP–O bond orbital also decreases. In contrast, in PEP and *o*-PC the variations are different: p character of P atom decreases and p character of O atom increases. The polarisation coefficient (P) increases from hydrated PO_4^{3-} to $H_2PO_4^-$ complex and the polarisation coefficient (O) decreases. In the hydrated PEP and *o*-PC complexes the polarisation coefficient (P) slightly decreases and the polarisation coefficient (O) increases. In all hydrated compounds,

Table 6
Relative energy (ΔE) (in Hartree and kcal/mol); total energy (E_{SCF}) (in Hartree) for all studied compounds at different level of theory

	E_{SCF} (1)	E_{H_2O} (2)	E_{SCF} (1+2)	E_{SCF}	ΔE (Hartree)	ΔE (kcal/mol)
B3LYP/6-31G*						
PO_4^{3-}	−641.8124	−76.4090	−718.2214	−718.3294	−0.1080	−67.77
HPO_4^{2-}	−642.8175	−76.4090	−719.2265	−719.2883	−0.0618	−38.78
$H_2PO_4^-$	−643.5876	−76.4090	−719.9966	−720.0285	−0.0319	−20.01
PEP	−909.5592	−76.4090	−985.9682	−985.9998	−0.0316	−19.83
o-PC	−778.0981	−76.4090	−854.5071	−854.5226	−0.0155	−9.73
B3LYP/6-311++G**						
PO_4^{3-}	−642.0874	−76.4585	−718.5459	−718.6247	−0.0788	−49.45
HPO_4^{2-}	−643.0178	−76.4585	−719.4763	−719.5265	−0.0502	−31.50
$H_2PO_4^-$	−643.7536	−76.4585	−720.2121	−720.2376	−0.0255	−16.00
PEP	−909.7985	−76.4585	−986.2570	−986.2806	−0.0236	−14.80
o-PC	−778.2873	−76.4585	−854.7458	−854.7584	−0.0126	−7.91

when the valence non-Lewis increases, the Rydberg non-Lewis increases too. In the phosphate compounds, when the occupancies of the localised σP–O orbital decrease, no definite trend is observed. In PEP and *o*-PC complexes the occupancies of the localised σP–O orbital increase when the occupancies of the localised σ*P–O orbital increase. In all cases the same variations are observed when the 6-311++G** basis set is used.

The smaller occupation for 6-31G* basis set in σP–O and σ*P–O orbitals implies a smaller P–O distance. Hence, the P–O bound value in the hydrated *o*-PC complex, is 1.4890 Å and the occupancy of σ*P–O orbital is 0.11526 while in the hydrated PO_4^{3-} complex the P–O distance is 1.6131 Å because the occupancy of the localised σP–O orbital is 1.97755. This observation does not change when the 6-311++G** basis set is used.

The NBO analysis reveals that in PO_4^{3-} complex the internuclear interaction of charge transfer from the O lone pair to the σ*P–O is stronger than in the other complexes. As a consequence, the occupation number of the antibonding orbital is fairly high. In all complexes, when the 6-311++G** basis set is used, the occupation of the σP–O orbital increases as follows: PO_4^{3-} (H_2O) > HPO_4^{2-} (H_2O) > $H_2PO_4^-$ (H_2O) > *o*-PC (H_2O). The occupation of the σ*P–O orbital decreases in the same direction, as seen in Table 5. Here again the exception in the PEP complex could be explained because the p character of P atom decreases while the p character of O atom increases.

3.3. Stability energies

Table 6 shows the relative energy for all studied complexes at different levels of theory, ΔE (in kcal/mol) is expressed in a similar form to that calculated by Reed et al. [22]. This is the difference between calculated energy for the hydrated complex (E_{SCF}) and the sum between the unhydrated complex [1] and one water molecule [2]. The total energy (E_{SCF}) is expressed in Hartree. The most important observations are the similar relative energy in the two basis sets for the hydrated $H_2PO_4^-$ and PEP complexes and the higher value of the relative energy for the hydrated *o*-PC complex. For this last reason, the *o*-PC (H_2O) is the most unstable hydrated complex. The lower relative energy value for PO_4^{3-} (H_2O) complex implies that this compound is a more stable complex than the others studied. For all complexes, when the 6-311++G** basis set is used, a notable decrease of the relative energy values is observed. The greatest variation observed in PO_4^{3-} (H_2O) is 18.32 kcal/mol; in HPO_4^{2-} (H_2O) it is 7.28 kcal/mol; in $H_2PO_4^-$ (H_2O) it is 15.8 kcal/mol; in PEP^- (H_2O) it is 5.03 kcal/mol and in *o*-PC (H_2O) it is 1.82 kcal/mol.

Table 7 shows the stabilisation energies for the studied compounds using the B3LYP method with 6-31G* and 6-311++G** basis sets. These are associated with the delocalisation from σP–O bond orbital to σ* P–O orbital, represented by σP–O→ σ* P–O, with the delocalisation from lone pairs to σ* O–H orbital, represented by LP(1–3)O → σ* P–O and with the delocalisation from lone pairs to σ*O–H orbital, represented by LP(1–3)O → σ* O–H. The last two transitions are known as charge transfer n → σ* P–O and n → σ* O–H. The σP–O → σ* P–O transition follows the trend: PO_4^{3-} (H_2O) > HPO_4^{2-} (H_2O) > $H_2PO_4^-$ (H_2O) whereas this transition for PEP (H_2O) is not observed. The n → σ* P–O transitions increase from PO_4^{3-} (H_2O) to $H_2PO_4^-$ (H_2O) and they are not observed for *o*-PC complex. The n → σ* O–H charge transfer decreases from PO_4^{3-} (H_2O) to $H_2PO_4^-$ (H_2O), whereas they have greater values in the PEP (H_2O) than in the *o*-PC (H_2O) complex. The total values of the stabilisation energies indicate that the PO_4^{3-} (H_2O) complex is more stable than the other complexes. The probable presence of the second H-bond of low energy in the hydrated *o*-PC and in the PEP complexes corresponding to n → σ* O–H and n → σ* H–C transitions (4.64 and 14.30 kcal/mol, respectively, with 6-31G* basis set and 1.64 and 4.74 kcal/mol, respectively, with 6-311++G** basis set) would stabilise these hydrated complexes. The presence of the greater value of the n → σ* O–H transition in PO_4^{3-} (H_2O) (37.14 kcal/mol) could stabilise the complex. Note that when the 6-311++G** basis set is used; the stabilisation energies have lower values in all cases. In addition, the same trend, as in the above case is observed with a variation of 10.61 kcal/mol in PO_4^{3-} (H_2O), 15.71 kcal/mol in HPO_4^{2-}(H_2O), 10.06 kcal/mol in $H_2PO_4^-$ (H_2O), 9.98 kcal/mol in PEP (H_2O) and 11.42 kcal/mol in *o*-PC (H_2O). The observed total stabilisation energies follow the sequence: PO_4^{3-} (H_2O) > HPO_4^{2-} (H_2O) > $H_2PO_4^-$ (H_2O) > *o*-PC (H_2O) (Table 6). The PEP (H_2O) complex has stabilisation energy comparable to the one of the phosphate complex because it has two H-bonds as will be seen later.

Table 7
Stabilisation energies (in kcal/mol) associated with delocalisation from σP—O bond orbital, lone pairs and delocalisation to σ*P—O bond orbital, represented by (σP—O→) and (σ*P—O→), respectively

PO_4^{3-} (H_2O)		HPO_4^{2-} (H_2O)		$H_2PO_4^-$ (H_2O)		PEP (H_2O)		o-PC (H_2O)	
B3LYP/6-31G*									
σP—O → σ*P—O	3.20	σP—O → σ*P—O	2.92	σP—O → σ*P—O	1.53				
LP(2)O → σ*P—O	10.05	LP(2)O → σ*P—O	14.24	LP(3)O → σ*P—O	15.27	σP—O → σ* O—H	0.65	σP—O → σ*P—O	5.76
LP(3)O → σ*P—O	9.25	LP(3)O → σ*P—O	12.66	LP(3)O → σ* O—H	6.57	LP(1)O5 → σ* O15–H16	8.57	σP—O → σ* O—H	0.24
LP(3)O → σ* O—H	37.14	LP(3)O → σ* O—H	14.46			LP(3)O5 → σ* O15–H16	23.13	LP(1)O2 → σ* O19–H18	6.29
	59.64		44.28		23.37	LP(3)O15 → σ* O2–H3	14.30	LP(2)O17 → σ*H9–C8	4.64
							46.65		16.93
B3LYP/6-311++G**									
σP—O → σ*P—O	1.81	σP—O → σ*P—O	1.27	σP—O → σ*P—O	1.53	σP—O → σ* O—H	0.08	σP—O → σ*P—O	0.00
LP(2)O → σ*P—O	8.91	LP(2)O → σ*P—O	9.37	LP(3)O → σ*P—O	11.78	LP(1)O5 → σ* O15–H16	5.69	σP—O → σ* O—H	0.00
LP(3)O → σ*P—O	9.63	LP(3)O → σ*P—O	9.37	LP(3)O → σ* O—H	3.65	LP(3)O5 → σ* O15–H16	16.60	LP(1)O2 → σ* O19–H18	3.87
LP(3)O → σ* O—H	23.99	LP(3)O → σ* O—H	8.59			LP(3)O15 → σ* O2–H3	4.74	LP(2)O17 → σ*H9–C8	1.64
	44.34		28.60		16.96		27.11		5.51

3.4. Topological analysis

The AIM theory is useful to investigate the inter and intramolecular interactions. In these cases, both inter and intramolecular interactions have been analysed by using Bader's topological analysis of the charge electron density, $\rho(r)$. The localisation of the critical points in the $\rho(r)$ and the values of the Laplacian at these points are important for the characterisation of molecular electronic structure in terms of interaction nature and magnitude. This critical point has the typical properties of the closed–shell interaction. That is, the value of $\rho(r)$ is relatively low, the relationship, $|\lambda 1|/\lambda 3$ is <1 and the Laplacian of the electron density, $\nabla^2\rho(r)$, is positive indicating that the interaction is dominated by the contraction of charge away from the interatomic surface toward each nucleus [32–39]. It is necessary to clarify that in this study, only the 6-311++G** basis set has been considered because there are numerous references where the quality of the basis set has no influence on the topological results [40,41]. Moreover, particularly in this case, for all complexes no significant variations are observed between 6-31G* and 6-311++G** basis sets.The details of the molecular models for all compounds studied showing the geometry of all their critical points may be asked from the authors upon request. The analyses of the O···H bond critical points in the compounds studied are reported for the hydrated phosphate complexes with the 6-311++G** basis set in Table 8. The electron densities at the critical points related to possible H-bonds: O2···H8 and O3···H7 bond in PO_4^{3-} (H_2O); O4···H9 and O5···H8 bond in HPO_4^{2-} (H_2O) and O3···H10 and O4···H9 bond in $H_2PO_4^-$ (H_2O), are between 0.02 and 0.05 a.u., which compares well with the values

Table 8
Analysis of the bond critical points in the compounds studied

B3LYP/6-311++G**					
PO_4^{3-} (H_2O)					
Bond	P1–O2	P1–O3	O···H	O6–H7, O6–H8	(3, +1)
$\rho(r)$	0.1790	0.1917	0.0533	0.2929	0.0156
$\nabla^2\rho(r)$	0.6388	0.8000	0.1296	**−0.45081**	0.0700
λ1	−0.2959	−0.3290	−0.0857	1.3251	−0.0131
λ2	−0.2946	−0.3273	−0.0833	−1.3148	0.0392
λ3	1.2297	1.4768	0.2988	0.836	0.0440
$\|\lambda 1\|/\lambda 3$	0.2406	0.2258	0.2900	**1.5850**	0.2980
HPO_4^{2-} (H_2O)					
Bond	P1–O4	P1–O5	O···H	O7–H8, O7–H9	(3, +1)
$\rho(r)$	0.1990	0.3534	0.0364	0.3202	0.0120
$\nabla^2\rho(r)$	1.1732	**−1.7912**	0.0977	**−1.6530**	0.0612
λ1	−0.3571	−1.6620	−0.0507	−1.5823	−0.0100
λ2	−0.3410	−1.6374	−0.0499	−1.5552	0.0281
λ3	1.8715	1.5080	0.1982	1.4860	0.0429
$\|\lambda 1\|/\lambda 3$	0.1908	**1.1021**	0.2442	**1.0648**	0.2330
$H_2PO_4^-$ (H_2O)					
Bond	P1–O3	P1–O4	O···H	O8–H9, O8–H10	(3, +1)
$\rho(r)$	0.2181	0.1533	0.0236	0.3396	0.0088
$\nabla^2\rho(r)$	1.456	0.5944	0.0696	**−1.7988**	0.0440
λ1	−0.3909	−0.2514	−0.0291	−1.6856	−0.0070
λ2	−0.3873	−0.2383	−0.0285	−1.6519	0.0146
λ3	2.2356	1.084	0.1272	1.5387	0.0365
$\|\lambda 1\|/\lambda 3$	0.1785	0.2319	0.2286	**1.0954**	0.1916

The quantities are in atomics units. The bold values are explained in the text.

Table 9
Analysis of the bond critical points in hydrated Phosphoenolpiruvate and Phosphocholamine studied

B3LYP/6-311++G**						
Bond	P1–O5	O···H	O2-H3	O5···H16	(3, +1)	(3, +1)
PEP (H_2O)						
$\rho(r)$	0.1363	0.0204	0.2247	0.0474	0.0109	0.0103
$\nabla^2\rho(r)$	0.4040	0.0593	1.5684	0.1424	0.0576	0.0528
λ1	−0.2048	−0.0262	−0.4061	−0.0769	−0.0103	−0.0066
λ2	−0.1899	−0.024	−0.3948	−0.0756	0.0256	0.0141
λ3	0.7990	0.1096	2.3694	0.2949	0.0423	0.0454
|λ1|/λ3	0.2563	0.2390	0.1714	0.2608	0.2435	0.1452
Bond	P1–O2	O17···H9	C8–H9	O···H	(3, +1)	
O–PC (H_2O)						
$\rho(r)$	0.1797	0.3666	0.2851	0.0101	0.0046	
$\nabla^2\rho(r)$	0.7116	**−2.4784**	**−0.9876**	0.0340	0.0200	
λ1	−0.3272	−1.7681	−0.7867	−0.0096	−0.0034	
λ2	−0.3083	−1.7284	−0.7549	−0.0938	0.0072	
λ3	1.3472	1.0180	0.5537	0.0531	0.0161	
|λ1|/λ3	0.2428	**1.7368**	**1.4208**	0.1807	0.2101	

The quantities are in atomics units. The bold values are explained in the text.

reported for different H-bonds compounds [34,36], where this quantity was found to vary from 0.022 to 0.044 a.u. In all H-bonds mentioned above, the Laplacian values are between 0.034 and 0.140 a.u., and compare satisfactorily with previous results [34,36]. The negative values of the Laplacian of the electron density for the O–H bond of water molecules of the phosphate complexes, observed in Table 8, indicate that the O–H bond critical points are not found in a region of charge depletion. The interaction O···H is different from the one encountered in the O–H bond of water and in P–O bond, which has of the shared interaction, i.e. the value of electron density at the bond critical point is relatively high, the relationship |λ1|/λ3 is greater than 1, and the Laplacian of the charge density is negative indicating that the electronic charge is concentrated in the internuclear region (bold values in the Table 8). The O···H bonds in PO_4^{3-} (H_2O); HPO_4^{2-} (H_2O) and $H_2PO_4^-$ (H_2O) complexes have typical properties of the closed–shell interaction because the $\rho(r)$ values are relatively low, the relationship, |λ1|/λ3<1 and the Laplacian of the electron density, $\nabla^2\rho(r)$, are positive. Moreover, the (3, +1) critical point in the hydrated phosphate would confirm the H-bond in the respective structures, as shown in Table 8. Those parameters are greater in PO_4^{3-} (H_2O) and in consequence the H-bond could be stronger in this complex than the other phosphates. Table 9 shows the analysis of the O···H bond critical points in PEP (H_2O) and *o*-PC (H_2O) complexes with the 6-311++G** basis set. The electron density values at the critical points related to possible H-bonds: O5···H16 and O15···H3 bond in PEP (H_2O) and O2···H18 and O17···H9 bond in *o*-PC (H_2O), vary between 0.050 and 0.010 a.u., while the relationship, |λ1|/λ3 < 1 and the Laplacian of the electron density, $\nabla^2\rho(r)$, are positive for the PEP complex. For the *o*-PC complex the corresponding critical point of the O17···H9 bond has values of |λ1|/λ3 > 1 and negative for $\nabla^2\rho(r)$. For this reason the H-bond O19···H9 is not formed although it was observed with the NBO analysis (nO17 → σ* H9–C8) (1.64 kcal/mol) with a lower stabilisation energy than the other transition observed (n → σ*O2–H3) (3.87 kcal/mol) (see Table 7). The only transition is confirmed by the presence of one (3, +1) critical point. The most significant results were obtained in the hydrated PEP complex due to other intermolecular H-bonds, that are confirmed by the presence of two (3, +1) critical points. In the hydrated PEP complex, the NBO analysis and the AIM program confirm that the charge transfer values from the lone pair of the oxygen (O5) to σ* O15–H16 is greater than the other transition observed (nO15 → σ* O2–H3) (see Tables 7 and 9) and for this reason the hydrated PEP complex is more stable than the hydrated *o*-PC complex.

The topological properties of $\rho(r)$ and $\nabla^2\rho(r)$ of the O atom of the water molecule give a similar trend to the ones observed for total energies: PO_4^{3-} (H_2O) > HPO_4^{2-} (H_2O) > $H_2PO_4^-$ (H_2O) > PEP (H_2O) > *o*-PC (H_2O) (Table 6).

3.5. Vibrational wavenumbers

The PO_4^{3-} has T_d symmetry and 9 normal modes of vibration. In contrast, their hydrated complex has a C_{2v} symmetry, as was previously reported by other authors [1,2], with 18 normal modes of vibration. The corresponding normal modes are visualised in Table 10 compared with the observed bands in infrared spectra in solid ($Na_3PO_4{\cdot}12H_2O$) and aqueous solution phases [4,9]. The calculated frequencies obtained with the B3LYP method using the 6-31G* and 6-311++G** basis sets are compared with the bands obtained by other authors using the HF method with the 6-31G* and 6-31+G* basis sets [2] and the B3LYP method with 6-311+G** basis set [1]. The stretching frequencies obtained with B3LYP method are lower than the HF values, while the frequencies calculated with 6-311+G** and 6-311++G** basis sets are closer and lower than the experimental values in solid and aqueous solution phases.

The HPO_4^{2-} and HPO_4^{2-} (H_2O) have a similar symmetry, C_s, the first has 12 normal vibrational modes whereas their hydrated complex has 21 normal vibrational modes.

Table 10
Theoretically and experimental infrared bands of PO_4^{3-} and PO_4^{3-} (H_2O) complex

HF[a]				B3LYP[b]	B3LYP/6-31G*[c]		B3LYP/6-311++G**[c]		Experimental		
Mode	Sym	6-31G*	6-31+G*	6-311+G**	PO_4^{3-}	PO_4^{3-} (H_2O)	PO_4^{3-}	PO_4^{3-} (H_2O)	PO_4^{3-} solid[c]	PO_4^{3-} solution[d]	PO_4^{3-} solution[e]
ν_s OH	A_1	3522.3	3583.3			2967		3045	3558		
ν_a OH	B_2	3330.6	3478.9			2625		2820	3216		
δ HOH	A_1	1962.8	1914.3			1829		1707	1666		
wag HOH	B_1	1203.8	1160.7			1115		1074	1040		
ν PO_4	B_1	1110.1	1033.0	911	962	1022	845	915	1012	1007	1013
ν PO_4	A_1	1073.5	1012.4	889	962	978	845	890	1012	1007	1013
ν PO_4	B_2	999.8	959.3	828	962	892	845	821	1012	1007	1013
ν PO_4	A_1	925.8	909.3	795	816	819	790	795		942	936
ρ HOH	B_2	747.9	665.9			803		719	738		
τ_w HOH	A_2	689.3	676.6			695		719	695		
δ PO_4	A_1	618.8	594.5	517	538	552	493	514	550	568	554
δ PO_4	B_2	613.2	587.4	508	538	542	493	508	550	568	554
δ PO_4	B_1	599.0	575.8	496	538	526	493	494.	550	568	554
δ PO_4	A_1	459.2	437.5	395	378	430	348	393	410	412	415
δ PO_4	A_2	408.8	396.2	341	378	360	348	340	410	412	415
ν_s O···H	A_1	291.6	267.4			294		270	–		
ν_a O···H	B_2	174.8	150.4			163		69	–		
Trans HOH	B_1	54.2	59.0			52		58	–		

ν, stretching; δ, deformation; ρ, rocking; wag, wagging; τ_w, torsion; a, antisymmetric; s, symmetric.
[a] Pye et al. [2].
[b] Ebner et al. [1].
[c] This work.
[d] Preston et al. [4].
[e] Niaura et al. [9].

Table 11 shows the theoretical and experimental infrared bands of HPO_4^{2-} and HPO_4^{2-} (H_2O). The infrared spectra of the solid ($Na_2HPO_4{\cdot}12H_2O$) and aqueous solution phases were compared with the calculated by the B3LYP method using 6-31G* and 6-311++G** basis sets. In general, the calculated frequency values with 6-311++G** basis set are close to experimental values in solid and aqueous solution phases.

The $H_2PO_4^-$ was optimised with C_s symmetry while their hydrated form with C_2 symmetry. The first form has 15 normal vibrational modes and the second one has 24 normal vibrational modes. Table 12 shows the theoretical and experimental infrared bands of $H_2PO_4^-$ and $H_2PO_4^-$ (H_2O). Also, in this case the infrared spectra of the solid ($NaH_2PO_4{\cdot}H_2O$) and aqueous solution phases were compared with the calculated B3LYP method using 6-31G* and 6-311++G** basis sets. The experimental stretching frequencies of PO_2^- group in aqueous solution [4,9] are lower than the corresponding one in solid phase. The changes are consistent with weakening of the P–O bond due to presence of H-bond. The same behaviour for the two methods is only observed between the calculated frequencies for $H_2PO_4^-$ and the hydrated complex. In the other phosphate complexes the observed differences agree with the variations in the corresponding P–O distances above analysed in Section 3.1 (Tables 3 and 4). The theoretical and experimental infrared bands of the corresponding hydrated PEP and *o*-PC complexes are summarised in Tables 13 and 14. The PEP; PEP (H_2O); *o*-PC and *o*-PC (H_2O) were optimised with C_1 symmetry. In the hydrated complexes, only the normal modes of vibration corresponding to the phosphate group are considered. For PEP with one water molecule, the infrared spectrum of the solid is visualised in Fig. 1a and the infrared frequencies are compared with the calculated bands with B3LYP method using 6-31G* and 6-311++G** basis sets in Table 13. Fig. 1b shows the infrared spectrum of the solid *o*-PC without water molecule and the infrared frequencies are compared with the calculated bands for the two basis sets used in Table 14.

In all cases, the frequencies calculated using the 6-311++G** basis set, are lower than those obtained using the 6-31G* basis set.

3.6. The phosphate groups

The experimental values for the band of greater frequency of the PO stretching increase from PO_4^{3-} to $H_2PO_4^-$ and the bands in solution are lower than the corresponding ones in solid phase. This fact is related with the H-bond formation because the decrease in the P–O strength bond has as a consequence a frequency increase in its vibrational mode. The theoretical frequencies of PO_4^{3-} are lower than the hydrated complex, but this fact can simply be visualised as a result of the stabilisation of PO_4^{3-} which is unstable in vacuum and very stable in solid and aqueous solutions [1]. For phosphate compounds, the following order corresponding to greater frequency of P–O stretching is observed: $H_2PO_4^- > HPO_4^{2-} > PO_4^{3-}$. This observation agrees with the variation in the P–O distance as shown in Tables 3 and 4. For the $H_2PO_4^-$ and hydrated complex the frequencies are calculated at 1294 and 1269 cm^{-1} (6-311++G**), respectively; for HPO_4^{2-} and hydrated complex the frequencies are calculated

Table 11
Theoretically and experimental infrared bands of HPO_4^{2-} (H_2O)

B3LYP/6-31G*[a]				B3LYP/6-311++G**[a]		Experimental		
Mode	Sym	HPO_4^{2-}	HPO_4^{2-} (H_2O)	HPO_4^{2-}	HPO_4^{2-} (H_2O)	HPO_4^{2-} solid[a]	HPO_4^{2-} solution[b]	HPO_4^{2-} solution[c]
ν PO–H	A′	3705	3732	3835	3841	3605		
ν_s OH	A′		3994		3452	3429		
ν_a OH	A″		3298		3375	3371		
δ HOH	A′		1853		1749	1717		
ν_a PO_3	A′	1180	1191	1098	1122	1139	1078	1083.3
ν_a PO_3	A″	1152	1098	1084	1049	1074	1078	1083.3
δ POH	A′	1006	1017	974	990	995		989.6
wag HOH	A′		938		931	955		
ν_s PO_3	A′	924	926	898	907	866	989	
ν POH	A′	634	664	586	619	619	860	855.1
τ_w HOH	A″		636		584	579		
ρ HOH	A″		551		577	533		
δ PO_3	A″	524	524	491	499	512	539	
δ PO_3	A′	490	509	472	493	464		
δ PO_3	A′	480	487	460	475	450		
δ PO_3	A′	339	359	327	349	392	390	
δ PO_3	A′	338	328	320	319	302		
wag P—OH	A″	311	255	139	233	234		
ν_s O···H	A′		250		134	–		
ν_a O···H	A″		156		103	–		
Trans HOH	A′		35		55	–		

ν, stretching; δ, deformation; ρ, rocking; wag, wagging; τ_w, torsion. a, antisymmetric; s, symmetric.
[a] This work.
[b] Preston et al. [4].
[c] Niaura et al. [9].

Table 12
Theoretical and experimental infrared bands of $H_2PO_4^-$ (H_2O)

B3LYP/6-31G*[a]				B3LYP/6-311++G**[a]		Experimental		
Mode	Sym	$H_2PO_4^-$	$H_2PO_4^-$ (H_2O)	$H_2PO_4^-$	$H_2PO_4^-$ (H_2O)	$H_2PO_4^-$ Solid[a]	$H_2PO_4^-$ solution[b]	$H_2PO_4^-$ solution[c]
ν_s OH (PO_4)	A	3766	3767	3844	3847	3547		
ν_a OH (PO_4)	B	3766	3767	3844	3846	3523		
ν_a OH	B		3648		3709	3462		
ν_s OH	A		3623		3685	3462		
δ HOH	A		1814		1713	1672		
ν_a PO_2	B	1335	1300	1294	1269	1247	1152	
ν_s PO_2	A	1103	1104	1064	1066	1169	1075	1076.8
δ POH	B	1075	1072	1045	1040	1050		
δ POH	A	1058	1059	1030	1026	969		
ν_a POH	B	792	824	751	785	844	946	
ν_s POH	A	748	765	728	749	785	875	876.8
wag HOH	B		695		686	636		
δ PO_2	A	492	500	486	487	515	520	
δ PO_2	B	484	479	480	480	487		
τ_w HOH	B		463		435	452		
ρ HOH	A		435		428	423		
δ PO_2	B	415	425	423	427	411		
δ PO_2	A	365	354	387	373	396	380	
δ PO_2	A	310	330	316	323	327		
wag OH	B	296	285	300	285	302		
ν_s O···H	A		196		179	223		
wag OH	A	171	152	198	165			
ν_a O···H	B		113		67			
Trans HOH	B		23		34			

ν, stretching; δ, deformation; ρ, rocking; wag, wagging; τ, torsion; a, antisymmetric; s, symmetric.
[a] This work.
[b] Preston et al. [4].
[c] Niaura et al. [9].

Table 13
Theoretical and experimental infrared bands of phosphoenolpiruvate with one water molecule

Mode	B3LYP/6-31G*[a]		B3LYP/6-311++G**[a]		Experimental[a]
	PEP	PEP (H_2O)	PEP	PEP (H_2O)	PEP (H_2O)
ν_a OH		3772		3876	3588
ν OH (PO_4)	3761	3497	3841	3680	3531
ν_s OH		3152		3203	3457
δ HOH		1750		1674	1668
δ POH	1335	1363	1298	1286	1196
ν PO_2	1106	1253	1080	1172	1081
ν PO_2	1084	1081	1051	1057	1047
ρ HOH		985		938	937
ν POH	803	843	785	813	850
wag POH		760		714	717
ν PO–R	696	707	678	627	578
δ PO_4	533	532	528	523	536
δ PO_4	493	512	490	473	513
δ PO_4	460	472	453	450	474
δ PO_4	439	464	437	440	450
τ_w HOH		403		421	392[b]
wag HOH		337		326	335[b]
wag POH	345	309	359	240	285[b]
ν O5···H16		246		231	259[b]
ν O15···H3		176		109	130[b]

ν, stretching; δ, deformation; ρ, rocking; wag, wagging; τ, torsion. a, antisymmetric; s, symmetric.
[a] This work.
[b] Bands observed in Raman spectrum.

Table 14
Theoretical and experimental infrared bands of Phosphocholamine with one water molecule

Mode	B3LYP[a]		B3LYP[a]		Experimental[a]
	6-31G*		6-311++G**		*o*-PC
	o-PC	*o*-PC (H_2O)	*o*-PC	*o*-PC (H_2O)	Solid
ν_a OH	–	3801		3894	
ν OH (PO_4)	3762	3765	3837	3838	3485
ν OH (PO_4)	3759	3760	3835	3834	3485
ν_s OH		3614		3639	
δ HOH		1740		1633	
ν PO_2	1311	1280	1280	1272	1259
δ POH	1076	1076	1099	1098	1088
δ POH	1067	1061	1039	1038	1034
ν PO-R	1048	1036	1026	1028	1017
ν POH	955	960	937	941	941
ν POH	932	940	854	912	906
ν PO_2	858	861	832	859	860
δ PO_4	771	765	759	754	767
ρ HOH		652		623	
δ PO_4	521	523	520	523	534
δ PO_4	471	473	469	472	500
δ PO_4	448	448	448	448	468
δ PO_4	421	423	419	422	418
ρ POH	374	379	371	388	376
ρ POH	358	358	354	372	353
τ_w HOH		307			
wag OH	225	197	248	248	254
ν O2···H18		183		190	
ν O17···H9		98		76	

ν, stretching; δ, deformation; ρ, rocking; wag, wagging; τ, torsion; a, antisymmetric; s, symmetric.
[a] This work.

at 1098 and 1122 cm^{-1} (6-311++G**), respectively, and for PO_4^{3-} and the hydrated complex the frequencies are calculated at 845 and 915 cm^{-1} (6-311++G**), respectively. The theoretical frequencies of P–O stretching in phosphocholamine and hydrated complexes are 1280 and 1272 cm^{-1} (6-311++G**), respectively; and with the same basis set, they are greater than the corresponding one to phosphoenolpiruvate and its hydrated complex (1080 and 1172 cm^{-1}, respectively). The P–O distances related with those frequencies are 1.4890 and 1.4852 Å in *o*-PC complex with 6-31G* and 6-311++G** basis sets, respectively, whereas they are 1.5184 and 1.5137 Å in PEP complex with the same basis sets. A very important observation is related to P–O bonded to H atom or R group. The P–OH stretching frequencies are greater in the $H_2PO_4^-$ and its hydrated complex (751 and 785 cm^{-1} with 6-311++G** basis set) than the HPO_4^{2-} and its hydrated complex (586 and 619 cm^{-1} with 6-311++G** basis set), because in the $H_2PO_4^-$ (H_2O) complex, the P–O distance is 1.6664 Å (6-311++G**) while in HPO_4^{2-} (H_2O) complex is 1.7576 Å (6-311++G**). In the *o*-PC and its hydrated complex, the PO-R frequencies are 1026 and 1028 cm^{-1} (6-311++G** basis set) and are greater than the calculated for PEP and its corresponding hydrated complex (678 and 627 cm^{-1} using 6-311++G** basis set). This variation is in agreement with the values of the PO–R distance. In the PEP complex they are 1.7173 Å (6-31G*) and 1.7124 Å (6-311++G**) while in the *o*-PC complex they are 1.5877 Å (6-31G*) and 1.5844 Å (6-311++G**).

The theoretical frequencies for the hydrated $H_2PO_4^-$, PEP and *o*-PC complexes using a 6-311++G** basis set are very close to the corresponding experimental values in solid phases. This behaviour may be due to the fact that the infrared spec-

Table 15
Experimental and theoretical infrared bands of water at different level of theory

Normal modes	Experimental[a]	3LYP/6-31G*[b]	B3LYP/6-311++G**[b]
ν_a OH	3615	3850	3922
ν_s OH	3450	3728	3817
δ HOH	1640	1792	1603

ν, stretching; δ, deformation, a: antisymmetric, s: symmetric.
[a] Ref. [41].
[b] This work.

tra of these compounds were registered with the corresponding monohydrate solids and the calculations were carried out with one water molecule. For PO_4^{3-} and $H_2PO_4^-$ complexes the experimental frequency values are different from to the calculated ones because the infrared spectra were registered with a 12 water molecules solid.

3.7. The OH stretching in the water molecule

The experimental and theoretical infrared bands of the water molecule at different levels of theory are shown in Table 15. The normal vibrational modes corresponding to water molecules in all complexes are observed from Tables 10–14. The theoretical frequencies using the B3LYP method with 6-31G* and 6-311++G** basis sets, of OH stretching in PO_4^{3-}, HPO_4^{2-} complexes appear inverted with reference to the free water molecule [42]. However, these frequencies for $H_2PO_4^-$, phosphocholamine and phosphoenolpiruvate complexes are in the same sequence than the frequencies for the water molecule. This behaviour could be related to the formation of H-bond and its nature. The optimised structures of water molecules in phosphate complexes (Figs. 2–6) are bidentate while in PEP and *o*-PC complexes the water molecules are monodentate. On the other hand, the H-bonds (P–O···H) are stronger in the complexes with this trend: $PO_4^{3-} > HPO_4^{2-} > H_2PO_4^-$, and the frequencies of the O–H antisymmetric and symmetric stretchings of the water increase when the frequencies of the O···H stretchings decrease. The O···H distance in hydrated PO_4^{3-} using 6-31G* basis set is 1.6891 Å and with 6-311++G** basis set is 1.7155 Å, while the two O–H stretchings of the water are calculated with 6-31G* basis set at 2967 and 2625 cm^{-1}, respectively; and using 6-311++G**basis set they are calculated at 3045 and 2820 cm^{-1}, respectively. In the HPO_4^{2-} complex the O···H distances are 1.8513 Å (6-31G*) and 1.8824 Å (6-311++G**) and the calculated frequencies of O–H stretchings of the water with the same basis set are calculated at 3452 and 3375 cm^{-1}, respectively. For $H_2PO_4^-$ complex the O···H distances are 2.0375 Å (6-31G*) and 2.1033 Å (6-311++G**) while the O–H stretching of the water using 6-311++G** basis set are calculated at 3709 and 3685 cm^{-1}, respectively. The O···H distances in PEP complex with two basis sets are lower (1.6931 and 1.6992) than *o*-PC complex (1.8941 and 1.8641 Å) and the antisymmetric and symmetric stretching frequencies of the water follow the same trend. These frequencies in the PEP complex using 6-311++G** basis set are 3876 and 3203 cm^{-1}, while in the *o*-PC complex they are 3894 and 3639 cm^{-1}. In relation to H-bond, the O···H frequencies in PO_4^{3-} complex using 6-31G* basis set are calculated at 294 and 163 cm^{-1}, while in HPO_4^{2-} complex they are 250 and 156 cm^{-1}. In $H_2PO_4^-$ complex these stretching modes with the same basis set are calculated at 196 and 113 cm^{-1} while in PEP complex (246 and 176 cm^{-1}) they are greater than in the *o*-PC complex (183 and 98 cm^{-1}). When the 6-311++G** basis set is used, the O···H stretching modes follow the same tendency.

The variations observed in the frequency values of the P–O, O–H and water O–H stretchings are consistent with the weakening of the O···H. Another important observation is the significant change in the frequencies of HOH water deformation mode (Tables 10–14) when the basis set is changed from 6-31G* to 6-311++G**. Using the latter basis set, the water deformation mode decreases, in all cases, by about 76–122 cm^{-1}, and the greater variations are observed in the P–O stretching modes for PO_4^{3-} complex (107 cm^{-1}). In the remaining complexes, the frequencies of the P–O stretchings change between 32 and 81 cm^{-1}. Finally, the frequencies of the vibration normal modes of phosphocholamine complex are less affected by the change in the basis set as seen in Table 14.

4. Conclusions

The lowest value obtained for ΔE (B3LYP/6-31G*) in the hydrated phosphate (−67.77 kcal/mol) suggests that the accumulated charges on the O atoms increase the stability of the compound. On the other hand, when the charge on the O atoms decreases, the relative energy decreases at −38.78 kcal/mol for hydrated HPO_4^{2-} complex and at −20.01 kcal/mol for hydrated $H_2PO_4^-$. In PEP, having only one charge, the −19.83 kcal/mol value is approximately equal to that of the $H_2PO_4^-$ complex. The greater value would correspond to a neutral molecule such as phosphocholamine (−9.73 kcal/mol). The PO_4^{3-} has a higher charge transference to the H-bonds (−37.34 kcal/mol) and a lower distance PO···H (1.6891 Å) than the other phosphate complexes. Instead, phosphocholamine has the lowest value of charge transference (6.29 kcal/mol) and the highest value in the PO···H distance (1.8941 Å) of the *o*-PC complex.

The results reveal that the H-bond in the PO_4^{3-} complex is highly stable and the frequencies related to the PO bond become lower. Accordingly, the predicted order of the relative stability of the hydrogen bonding of the investigated compounds followed the order: $PO_4^{3-}(H_2O) > HPO_4^{2-}(H_2O) > H_2PO_4^-(H_2O) >$ PEP $(H_2O) >$ *o*-PC (H_2O).

These results confirm the general trend found for the interaction of an ion with the water molecule. It increases the charge transference in comparison with a neutral molecule such as *o*-PC. The most important observation that arises from the work is that the presence of H or R groups weakens the H bond.

Increasing the size of the basis set improves the results of the geometrical parameters and the vibrational frequencies, but not the relative energy values.

The results obtained with the AIM program are independent of the basis set used and they have shown that the analysis of the charge density in all compounds satisfy the criteria of hydrogen bonding interactions. Besides, we observed a good correlation between $\rho(r)$, $\nabla^2\rho(r)$ and the stability.

The relevance of these results and the corresponding theoretical analysis support the possibility that the hydration of the phosphate groups linked to acylglycerol moieties, such as the phospholipid constituting the biological membranes, can be regulated by the type of group esterified to it. The simplicity of the compounds chosen for this work and the conclusions derived from it, constitute an important step in the track to study regulatory properties of complex biologically relevant phosphate compounds, such as those found in biological membranes.

Acknowledgements

S.A. Brandán thanks the Beca Banco Rio for a grant supporting this work. This work was founded with grants from UBA-CyT (Ciencia y Técnica de la Universidad de Buenos Aires), CIUNT (Consejo de Investigaciones, Universidad Nacional de Tucumán), and CONICET (Consejo Nacional de Investigaciones Científicas y Técnicas, Argentina).

Appendix A. Supplementary data

Supplementary data associated with this article can be found, in the online version, at doi:10.1016/j.saa.2006.05.005.

References

[1] C. Ebner, U. Onthong, M. Probst, J. Mol. Liquids 118 (2005) 15.
[2] C.C. Pye, W.W. Rudolph, J. Phys. Chem. A 107 (2003) 8746.
[3] K. Range, M.J. McGrath, X. Lopez, D.M. York, J. Am. Chem. Soc. 26 (2004) 1654.
[4] C.M. Preston, W.A. Adams, J. Phys. Chem. 83 (7) (1979) 814.
[5] R. Caminiti, P. Cucca, D. Atzei, J. Phys. Chem. 89 (1985) 1457.
[6] P.E. Mason, J.M. Cruikshank, G.W. Neilson, P. Buchanan, Phys. Chem. Chem. Phys. 5 (2003) 4686.
[7] J.R. Rustad, D.A. Dixon, J.D. Kubicki, A.R. Felmy, J. Phys. Chem. A 104 (2000) 4051.
[8] A.C. Chapman, L.E. Thirlwell, Spectrochim. Acta 20 (1964) 937.
[9] G. Niaura, A.K. Gaigalas, V.L. Vilker, J. Phys. Chem. 101 (1997) 9250.
[10] V. Luzzati, F.J. Husson, J. Cell Biol. 12 (1962) 207.
[11] D. Chapman, R.M. Williams, B.D. Ladbrooke, Chem. Phys. Lipids 1 (1967) 445.
[12] J.N. Sachs, T.B. Woolf, J. Am. Chem. Soc. 125 (29) (2003) 8742.
[13] W. Hübner, A. Blume, Interactions at the lipid–water interface, Chem. Phys. Lipids 96 (1998) 96.
[14] W. Phole, C. Selle, H. Fritzsche, H. Binder, Biospectroscopy 4 (1998) 267.
[15] S.A. Brandán, S.B. Díaz, R. Cobos Picot, E.A. Disalvo, A. Ben Altabef, accepted for publication in Spectrochimica Acta Part A., 66 (2007) 1152.
[16] F. Lairon, E.A. Disalvo, Langmuir 20 (2004) 9151.
[17] E.A. Disalvo, F. Lairon, S. Diaz, J. Arroyo, Res. Signpost 37/66 (2) (2002), Trivandrum, Kerala, India.
[18] E.A. Disalvo, F. Lairon, F. Martini, H. Almaleck, S. Diaz, G. Gordillo, J. Arg. Chem. Soc. 92 (4–6) (2004) 1.
[19] F. Martini, E.A. Disalvo, Colloids Surf. B Biointerfaces 22 (2001) 219.
[20] J. Kim, G. Kim, P.S. Cremer, Langmuir 17 (2001) 7255.
[21] M.J. Frisch, G.W. Trucks, H.B. Schlegel, G.E. Scuseria, M.A. Robb, J.R. Cheeseman, V.G. Zakrzewski, J.A. Montgomery Jr., R.E. Stratmann, J.C. Burant, S. Dapprich, J.M. Millam, A.D. Daniels, K.N. Kudin, M.C. Strain, O. Farkas, J. Tomasi, V. Barone, M. Cossi, R. Cammi, B. Mennucci, C. Pomelli, C. Adamo, S. Clifford, J. Ochterski, G.A. Petersson, P.Y. Ayala, Q. Cui, K. Morokuma, D.K. Malick, A.D. Rabuck, K. Raghavachari, J.B. Foresman, J. Cioslowski, J.V. Ortiz, A.G. Baboul, B.B. Stefanov, G. Liu, A. Liashenko, P. Piskorz, I. Komaromi, R. Gomperts, R.L. Martin, D.J. Fox, T. Keith, M.A. Al-Laham, C.Y. Peng, A. Nanayakkara, C. Gonzalez, M. Challacombe, P.M.W. Gill, B. Johnson, W. Chen, M.W. Wong, J.L. Andres, C. Gonzalez, M. Head-Gordon, E.S. Replogle, J.A. Pople, Program GAUSSIAN 98, revision A.7, Gaussian, Inc., Pittsburgh, PA, U.S.A., 1998.
[22] A.E. Reed, L.A. Curtiss, F. Weinhold, Chem. Rev. 88 (1988) 899.
[23] J.P. Foster, F. Weinhold, J. Am. Chem. Soc. 102 (1980) 7211.
[24] A.E. Reed, F. Weinhold, J. Chem. Phys. 83 (1985) 1736.
[25] R.F.W. Bader, Atoms in Molecules—A Quantum Theory, Oxford University Press, Oxford, 1990, ISBN: 0198558651 (Available on-line from http://www.amazon.com).
[26] A.B. Nielsen, A.J. Holder, GaussView, User's Reference, GAUSSIAN, Inc., Pittsburgh, PA, USA, 1997–1998.
[27] A.D. Becke, Phys. Rev. A38 (1988) 3098.
[28] C. Lee, W. Yang, R.G. Parr, Phys. Rev. B41 (1988) 785.
[29] E.D. Glendening, J.K. Badenhoop; A.D. Reed, J.E. Carpenter, F.F. Weinhold, NBO 4.0, Theoretical Chemistry Institute, University of Wisconsin, Madison, WI, 1996.
[30] A. Ebrahimi, F. Deyhimi, H. Roohi, J. Mol. Struct. (THEOCHEM) 626 (2003) 223.
[31] F. Biegler-Köning; J. Schönbohm, D. Bayles, AIM 2000: A Program to Analize and Visualize Atoms in Molecules, J. Comput. Chem. 2001, 22, 545–559.
[32] R.F.W. Bader, J. Phys. Chem. A 102 (1998) 7314.
[33] P.L.A. Popelier, J. Phys. Chem. A 102 (1998) 1873.
[34] U. Koch, P.L.A. Popelier, J. Phys. Chem. 99 (1995) 9747.
[35] G.L. Sosa, N. Peruchena, R.H. Contreras, E.A. Castro, J. Mol. Struct. (THEOCHEM) 401 (1997) 77.
[36] G.L. Sosa, N. Peruchena, R.H. Contreras, E.A. Castro, J. Mol. Struct. (THEOCHEM) 577 (2002) 219.
[37] S. Wojtulewski, S.J. Grabowski, J. Mol. Struct. 645 (2003) 287.
[38] S. Wojtulewski, S.J. Grabowski, J. Mol. Struct. 621 (2003) 285.
[39] S.J. Grabowski, Monatshefte für Chemie 133 (2002) 1373.
[40] C. Vizioli, M.C. Ruiz de Azúa, C.G. Giribet, R.H. Contreras, L. Turi, J.J. Dannenberg, Y.D. Rae, J.A. Weingold, M. Malagoli, R. Zanasi, P. Lazzeretti, J. Phys. Chem. 98 (1994) 8858.
[41] J. Cioslowski, S.T. Mixon, W.D. Edwards, J. Am. Chem. Soc. 113 (1991) 1083.
[42] K. Nakamoto, Infrared and Raman Spectra of Inorganic and Coordination Compounds, fifth ed., J. Wiley & Sons, Inc., 1997.